Arab J. Nucl. Sci. Appl., Vol. 55, 4, 139-149 (2022)

ISSN 1110-0451

Arab Journal of Nuclear Sciences and Applications

Web site: ajnsa.journals.ekb.eg

(E S N S A)

Environmental Radioactivity Monitoring Using High Resolution Gamma-ray Spectrometer for Lake Manzala in Egypt

M. MITWALLI[1,2]*, C. DULAMA[3], M. SALLAH[1,4], D. CHIRLEŞAN[5], A. H. EL-FARRASH[1]

(1) Physics Department, Faculty of Science, Mansoura University, Mansoura 35516 Egypt

(2) National Network for Nuclear Sciences, Academy of Scientific Research and Technology (NNS-ASRT), 11334 Cairo, Egypt

(3) Radiation Protection Department, Institute of Nuclear Research, 115400 Pitesti, Romania

(4) Higher Institute of Engineering and Technology, New Damietta, Egypt

(5) Faculty of Sciences, University of Pitești, 110040 Pitești, Romania

ARTICLE INFO

Article history:

Received: 13th Apr. 2022

Accepted: 6th Aug. 2022

Keywords:

Environmental Radioactivity, Gamma-ray Spectrometer, HPGe, Radionuclides, Lake Manzala

ABSTRACT

The environmental radioactivity of the Lake Manzala, Egypt, has been investigated to determine the level of the natural radioactivity and the radiological impact for the targeted area. Twenty sediment samples were collected from pre-determined locations, which involve deep springs and lakes, particularly samples taken from places receiving sewage pollutants, fertilizers and disinfection materials used in the agricultural area and fish farms. The gamma-emitting nuclides library has been designed to assess the activity concentration for radionuclides belonging to the natural series of uranium and thorium (^{208}Tl, ^{212}Bi, ^{212}Pb, ^{214}Bi, ^{214}Pb, ^{226}Ra, ^{228}Ac, ^{234}Th, ^{235}U), and ^{40}K gamma-line. The measured overall average value of the radionuclides' activity concentration was 15 Bq/kg, while for ^{40}K was 286 Bq/kg. The true coincidence summing was corrected using the Genie-2000 software, and LabSOCS was used to calculate the total efficiencies. Most of the resulted values are moderated, indicating normal levels compared to the international and worldwide reference values in this regard.

INTRODUCTION

We inhale radionuclides from the air, soil, water, and food every day since natural radioactivity is common in rocks, especially in Uranium, coal, and mineral mines. Environmental radiation is due to various radioactive nuclides present in the sediment and rocks distributed depending on the region's geological and geographical features, so radionuclides have been present on the earth's surface [1-4]. Among the different isotopes of radon, focus is made on ^{222}Rn (with a half-life of 3.82 days), which decays into many short-lived isotopes. However, daughter progenies such as ^{218}Po and ^{214}Po are high alpha emitters [5-9]. Together with its daughter products, Radon is the highest contributor to human exposure to natural background radiation [1, 3, 4, 10, 11]. Radioactivity is the macroscopic expression of nuclear decay, which is the physical process occurring spontaneously, in a stochastic manner, when atomic nuclei of an isotope undergo internal transformations to achieve more stable energy states. The decay process is accompanied by the emission of nuclear particles or photons carrying the energy in excess. Thus, the radioactivity analysis is a complex process aiming at identifying and quantifying radioactive isotopes since nuclear radiation may occur in various types, abundances, and energies, which are characteristics of each radionuclide [10, 12, 13]. The specific levels of terrestrial environmental radiation are related to the geological composition of each lithologically separated area and the content of natural radionuclides in sediment soil originating in each area [13]. Outstanding differences in natural radioactivity of soils can exist in relation to their geological origin and estuaries in Lake Manzala, Egypt [13-15]. Therefore, natural radionuclides used to differentiate investigated areas are based on deep springs and lake estuaries. The altitudes of the sampling areas influence the activity concentrations of uranium and thorium isotopes.

Ecosystems on higher altitudes are predisposed to receive more fallout and, therefore, higher concentrations of these radionuclides [15]. Lake Manzala is Egypt's most important shoreline lake [16, 17]. It is the biggest lake from the northern part of the Nile Delta, and is located in an area delimited by longitudes between 31˚ 50'E and 32˚ 15' E and latitudes between 31˚ 00'N and 31˚ 35' N. The area covered by Lake Manzala is of about 1071 km^2, with a maximum length of 64.5 km, and the maximum width of 49 km.

Corresponding author: meto_mms@yahoo.com

DOI: 10.21608/ajnsa.2022.133108.1569

Due to the fact that Manzala Lake is the largest of the Nile delta lakes, it has great economic value that appears in the fields of medicinal, human food, timber, fuel and other uses. In addition, it attributed to the increase of the fish farms around it. Deposit of the area of the Lake has been reduced effectively; its importance increased; as it is connected to the Mediterranean Sea and Suez Canal, in addition to many drains. Additionally, Lake Manzala is characterized by a large number of islets (about 1022) comprising approximately 180 km^2. All these factors give it a particular importance. It is worth noting why a project was launched in 1997-1999 by the Egyptian government, with financial support from the Global Environment Facility (GEF), to clean up the polluted water of Bahr El-Baqar drain to reduce the pollution of Lake Manzala and the Mediterranean Sea [18].

Moreover, it can represent a sustainable source of water in the residential area. Hence, it is necessary to assess the radioactivity level and radiological impact of the Lake Manzala because it receives an excessive load of various polluted wastewaters, including sewage water and chemical fertilizers used in the surrounding farmland, which in turn works to raise the distribution pattern of heavy metals in the Lake Manzala aquatic ecosystem [17, 19]. Recently, natural radioactivity has been inceaed as a source to human pollution coming from artificial radioactive contamination [17, 20]. The present study aims at assessing and estimating the environmental radioactivity burden characterizing the Lake Manzala due to the constantly received excessive load of diverse polluted wastewaters, including sewage water and chemical fertilizers. Therefore, it was also important to make an environmental monitoring synchronized with the changes occurring in the aquatic ecosystem and the sediments concentrated at the Lake's bottom. According to the IAEA protocols [21], predetermined 20 samples have been collected to cover the studied area. The radioactivity assessment has been carried out in the Radiation Protection Department of RATEN-ICN, Romania, using the HPGe spectrometer.

MATERIALS AND SAMPLING

For the sake of the current study, 20 sediment samples were collected from Lake Manzala and its surrounding areas. Table (1) and Fig. (1) show the stations and descriptions for each sample collected from investigated area. The sampling procedures followed the IAEA protocols mentioned in TECDOC-1415 [21] and the Egyptian Geological Survey and Mining Authority recommendations. The investigation sediment samples were stored in the open air for 4 days and then were dried in an electric oven at 110°C for 3 hours. All samples were grinded and avoided contamination by cleaning the grinding bowl with ethylene each time, and then, the samples were sieved to obtain a fine powder. Sample aliquots were weighted and stored for 27 days in sealed polyethylene cylindrical containers, namely Sarpagan, of 10 cm in diameter and 3 cm high. It is usually assumed that the dose rate does not change over the period of burial, implying that the uranium and thorium decay series are in secular equilibrium [22]. Therefore long radioactive half-lives, ^{238}U and ^{234}U isotopes are in secular equilibrium in all minerals and rocks greater than one million years old in a closed system or undisturbed minerals since ^{234}U is a daughter product of ^{238}U and the activity ratio (AR) of ^{234}U to ^{238}U is unity in the bulk of such materials. However, when such rocks, sediments and minerals have interacted with groundwater, the ratio may deviate from unity on either side; disequilibrium is the result depending on the geochemical conditions [5, 7, 23-25]

Table (1): Stations and description of investigated samples collected from Lake Manzala and its surrounding area

Sample	Investigated Station
M1	Damietta, near to El-Husania city.
M2	El-Rodah, the flow of the Faraskour drain into the lake.
M3	El-Serw, the flow of the El-Serw drains into the lake.
M4	El-Gamalyia, the flow of the El-Gamalyia drain into the lake.
M5	Lissa El-Gamalyia, close to Island drain and bar El-Ezby Soliman.
M6	The clear water area in the middle of the lake.
M7	El-Nassima 1, end of the long drain mixing with lake water.
M8	Bahr El-Baqar 1, end of Bahr El-Baqar drain at the lake water.
M9	El-Mataria, close to the El-Mataria drain outlet
M10	End of Hados drain mixing with lake water.
M11	Ibn Salam Island, near to El-Mataria city.
M12	El-Legan, the area with clear water from the middle of the lake.
M13	Bahr El-Baqar 2, About 10 Km away from Port Said Road.
M14	Port Said, near Port Said Canal.
M15	El-Hamra, an area of Brackishwater near the Mediterranean Sea.
M16	El-Ghamil, boughaz bridge linked with the Mediterranean Sea.
M17	Fiala Island, near Port Said
M18	Kassab Island, the mid of the lake.
M19	El-Nassima 2, the mid of the lake.
M20	El-Tabia, about 5 Km away from the international coastal road.

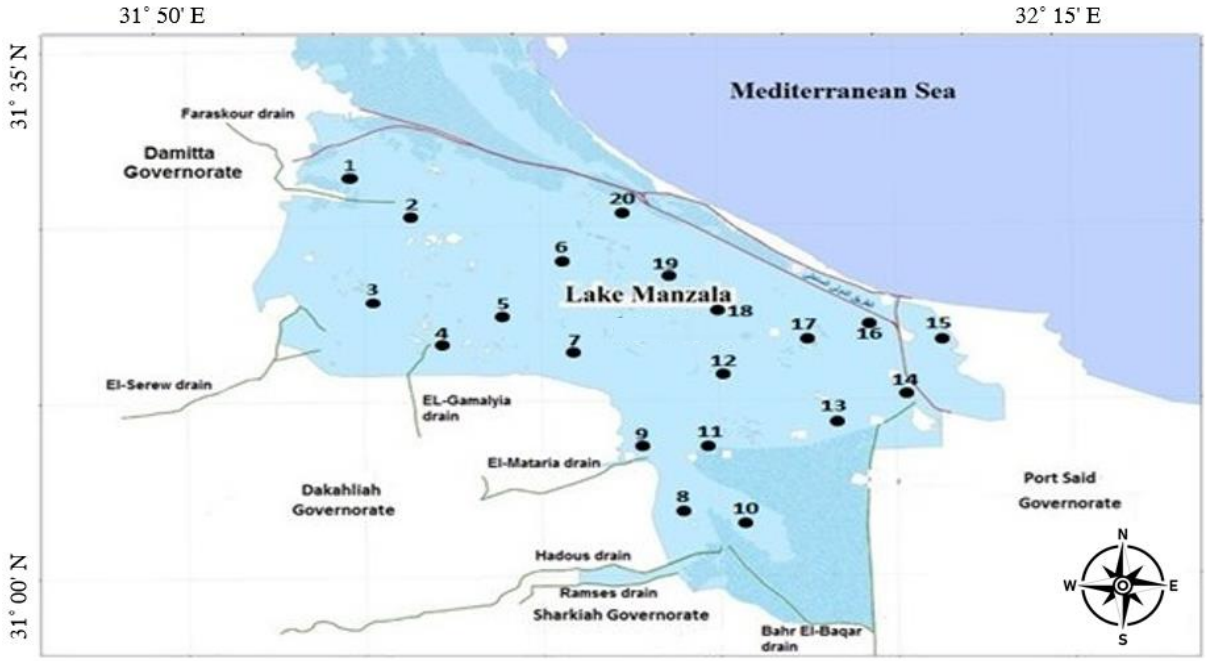

Fig. (1): Map of the distribution pattern of collected samples of Lake Manzala, *Egypt*

Experimental Technique

The samples have been analyzed using a high-resolution gamma spectrometer consisting of a 25% relative efficiency P-type coaxial HPGe detector and a Canberra Inspector 1270 integrated spectroscopy workstation. The spectra have been analyzed with Genie-2000 version 3.1 software, including the gamma analysis option. The gamma-emitting nuclides library has been designed to assess the activity concentration for radionuclides belonging to the natural series of Uranium and thorium, as ^{208}Tl, ^{212}Bi, ^{212}Pb, ^{214}Bi, ^{214}Pb, ^{226}Ra, ^{228}Ac, ^{234}Th, ^{235}U, and ^{40}K [5, 26-32], respectively. The efficiency calibrations used have been conducted using a multi-nuclide standard solution and identical source containers similar to those used for the analysis of the samples. No density corrections have been applied due to the narrow range of apparent densities of the analyzed samples, with values close to 1 g/cm^3.

True coincidence summing has been corrected using the Genie-2000 software, and LabSOCS calculated the total efficiencies. The gamma-emitting nuclides library has been designed to include ^{40}K and all gamma-emitters belonging to the natural uranium and thorium series. The sample containers used were cylindrical plastic boxes with a diameter of 10 cm and a height of 3 cm, filled with around 150 cm^3 of sample material.

RESULTS AND DISCUSSION

The obtained data from radioanalytical measurements are presented in Tables (2 and 3), and for signifying the radioactivity level of the investigated area, the results of the current study were compared with similar lakes in Egypt and others worldwide in Table (4). The activity concentration of ^{235}U ranged between 1.2 and 2.5 Bq/kg, with an average of 1.7 Bq/kg, corresponding to the natural uranium concentration (between 2.1 and 4.3 mg/kg). For comparison, in Europe, the median uranium concentration in sediments is estimated to be approximately 2 mg/kg, with a range of variation from less than 1 to more than 90 mg/kg [7-9, 33]. The activity concentration of ^{226}Ra ranged between 20.3 and 47.5 Bq/kg, with an average of 30.2 Bq/kg. As a reference, the average worldwide population-weighted value for ^{226}Ra concentration in sediment soil is 32 Bq/kg [10].

Furthermore, for North Africa (Egypt) a reference interval for ^{226}Ra concentration in soil was found to be between 5 and 64 Bq/kg, with an average value of 17 Bq/kg [21]. ^{228}Ac is a decay product of ^{232}Th; therefore, its activity concentration in environmental samples should be linked to the level of concentration of its parent. For the analyzed sediment samples, the specific activity of ^{228}Ac ranged between 7.0 and 22.9 Bq/kg, with an average of 16.1 Bq/kg.

Assuming radioactive equilibrium with ^{232}Th, the activity concentrations of ^{228}Ac translate into a thorium concentration between 1.7 and 5.6 mg/kg, with an average value of 3.9 mg/kg. As a reference, a worldwide average value of 45 Bq/kg can be considered for ^{232}Th activity concentration in soil [4]. Finally, the activity concentration of ^{40}K ranged is between 127.6 and 409.1 Bq/kg, with an average value of 285.8 Bq/kg, well below the world average level of 420 Bq/kg [7, 8, 34].

The comparison between the activity concentration values of ^{238}U gamma-emitting daughter nuclides (^{214}Bi, ^{214}Pb, ^{226}Ra, and ^{234}Th) is shown in Fig. (2). One can observe that while ^{234}Th and ^{226}Ra activity concentrations are close to each other in most of the samples, they differ significantly from the corresponding values of activity concentrations of ^{214}Bi and ^{214}Pb. This is due to the broken equilibrium in the decay chain and ^{222}Rn escape from the sample containers.

Table (2): The activity concentration (Bq/kg) of ^{238}U, ^{235}U natural series, and ^{40}K for sediment investigation samples using the gamma line spectra measured by HPGe spectrometer

Code	Activity Concentration Bq/kg					
	^{40}K	^{235}U	^{238}U			
			^{214}Bi	^{214}Pb	^{226}Ra	^{234}Th
M1	340.1 ± 32.4	< 1.5*	12.6 ± 1	16.1 ± 1.1	< 26.1*	18.4 ± 3.1
M2	409.1 ± 59.2	< 1.6*	15.6 ± 1.5	16.0 ± 1.1	< 26.8*	< 31.7*
M3	256.8 ± 24.8	1.7 ± 0.5	10.4 ± 0.9	11.3 ± 0.9	32.7 ± 5.2	21.7 ± 3.6
M4	368.8 ± 53.5	1.7 ± 0.6	12.7 ± 1.3	14.4 ± 1.1	32.7 ± 1.7	< 31.6*
M5	127.6 ± 13.6	2.2 ± 0.7	6.7 ± 1	9.5 ± 0.9	41.4 ± 6.7	41.6 ± 4.7
M6	209.5 ± 31.9	1.7 ± 0.6	7.5 ± 1.3	8.7 ± 0.9	32.3 ± 5.1	42.3 ± 9.5
M7	240.6 ± 23.2	< 1.6*	8.0 ± 0.9	10.9 ± 0.8	< 27.6*	23.2 ± 3.8
M8	401.3 ± 58	< 1.4*	14.6 ± 1.4	14.9 ± 1.1	< 24.3*	< 29.9*
M9	226.9 ± 22.1	< 1.8*	8.7 ± 0.9	11.0 ± 0.9	< 30.5*	25.0 ± 3.6
M10	225.2 ± 33.7	1.7 ± 0.5	7.9 ± 1.2	10.1 ± 0.9	33.1 ± 1.7	< 33.3*
M11	248.5 ± 24.1	2.5 ± 0.6	8.7 ± 0.9	12.2 ± 0.9	47.5 ± 7.6	39.9 ± 4.6
M12	273.6 ± 40.2	1.5 ± 0.5	12.2 ± 1.3	13.7 ± 1.0	29 ± 4.6	< 30.8*
M13	317.9 ± 30.3	< 2.1*	9.2 ± 0.9	11.7 ± 0.8	< 36.6*	23.2 ± 3.5
M14	146.9 ± 24.2	< 1.7*	5.7 ± 1.7	6.9 ± 1.0	< 28.3*	< 37.8*
M15	281.1 ± 26.8	< 1.5*	12.5 ± 1	17.2 ± 1.1	< 25.3*	17.5 ± 3.3
M16	281.6 ± 41.2	< 1.4*	8.7 ± 1.0	9.8 ± 0.9	< 24.3	< 28.3*
M17	280.2 ± 26.6	< 1.3*	4.3 ± 0.6	6 ± 0.5	< 21.3*	< 7.1
M18	314.6 ± 45.8	< 1.2*	11.9 ± 1.3	10.3 ± 0.9	< 20.3*	< 28.8*
M19	381.4 ± 36.2	1.8 ± 0.5	14.7 ± 1.1	19.7 ± 1.2	34.9 ± 5.6	19.5 ± 3.4
M20	383.8 ± 55.6	< 1.6*	14.6 ± 1.3	16.2 ± 1.1	< 29.2*	< 30.7*
Min.	127.6 ± 13.6	< 1.2*	4.3 ± 0.6	6 ± 0.5	< 20.3*	< 7.1*
Max.	409.1 ± 59.2	2.5 ± 0.6	15.6 ± 1.5	19.7 ± 1.2	47.5 ± 7.6	42.3 ± 9.5
Ave.	285.8	1.7	10.3	12.3	30.2	28.1
St. Dev.	0.7	0.3	3.2	3.5	6.5	8.9
*Minimum Detectable Activity (MDA)						

Table (3): The activity concentration (Bq/kg) of ^{232}Th natural series for sediment investigation samples was measured using the gamma line spectra by the HPGe spectrometer

Code	Activity Concentration Bq/kg			
	^{232}Th			
	^{208}Tl	^{212}Bi	^{212}Pb	^{228}Ac
M1	7 ± 0.6	22.2 ± 3.4	21 ± 1.3	19.7 ± 1.3
M2	6.8 ± 0.7	< 17.8	23 ± 1.5	21.9 ± 1.5
M3	5.1 ± 0.5	21.8 ± 3	16.5 ± 1.1	14.6 ± 1.0
M4	7.1 ± 0.7	24.4 ± 4.2	21.2 ± 1.4	21.1 ± 1.4
M5	2.8 ± 0.5	< 8.9*	9.4 ± 0.8	8.2 ± 0.9
M6	5.7 ± 0.7	20.5 ± 4.5	16.5 ± 1.2	15.7 ± 1.4
M7	5.1 ± 0.5	16.2 ± 2.9	15.2 ± 1	14.0 ± 1.0
M8	6.5 ± 0.7	28.4 ± 5.5	21.2 ± 1.4	17.8 ± 1.3
M9	5.4 ± 0.5	16.3 ± 3.4	16.9 ± 1.1	15.9 ± 1.1
M10	5.9 ± 0.7	16.8 ± 4.6	19.2 ± 1.3	16.7 ± 1.4
M11	5.3 ± 0.5	19.7 ± 3.4	17.8 ± 1.2	16.3 ± 1.1
M12	6.9 ± 0.7	24.6 ± 5.1	19.5 ± 1.3	17.1 ± 1.3
M13	6 ± 0.5	20.5 ± 3.2	17.9 ± 1.1	16.1 ± 1.1
M14	3.7 ± 0.7	< 21.9*	13.2 ± 1.0	12.5 ± 1.5
M15	6.8 ± 0.6	20.8 ± 2.9	20.6 ± 1.3	17.7 ± 1.1
M16	4.7 ± 0.6	15.4 ± 4.6	16 ± 1.1	13.5 ± 1.1
M17	1.9 ± 0.3	7.3 ± 1.8	6.6 ± 0.5	7.0 ± 0.6
M18	5.3 ± 0.6	24.6 ± 5.3	16.4 ± 1.1	14.6 ± 1.2
M19	7.2 ± 0.6	24 ± 3.3	23.3 ± 1.4	22.9 ± 1.4
M20	7.2 ± 0.7	26.3 ± 5.1	22.2 ± 1.5	18.6 ± 1.3
Min.	1.9 ± 0.3	7.3 ± 1.8	6.6 ± 0.5	7.0 ± 0.6
Max.	7.2 ± 0.7	28.4 ± 5.5	23.3 ± 1.4	22.9 ± 1.4
Ave.	5.6	19.9	17.7	16.1
St. Dev.	1.4	5.3	4.3	4
*Minimum Detectable Activity (MDA)				

Fig. (3) shows the activity concentration of ^{232}Th gamma-emitting daughter nuclides (^{208}Tl, ^{212}Bi, ^{212}Pb, and ^{228}Ac). A good agreement can be observed between the values of the activity concentrations for all these decay products, which is due to the secular equilibrium attained in the thorium series. In addition, Figures (4 and 5) show the comparison of descriptive statistical analysis for the obtained data.

Figures 6 (a, b, c, d, e, and f) illustrates the correlation between the activity concentration values of (^{226}Ra, and ^{235}U); (^{214}Bi and ^{214}Pb); (^{212}Bi and ^{212}Pb); (^{214}Bi and ^{212}Bi); (^{214}Pb and ^{212}Pb); (^{235}U and ^{234}Th), respectively. One can observe that a good correlation has been obtained for ^{226}Ra vs. ^{235}U, ^{212}Bi vs. ^{212}Pb, ^{214}Bi vs. ^{214}Pb, and ^{235}U vs. ^{234}Th, respectively, since these radionuclides belong either to the same series, including ^{214}Bi / ^{214}Pb and ^{212}Bi / ^{212}Pb, or to the linked series of natural uranium isotopes.

On the other hand, for ^{214}Bi vs. ^{212}Bi and ^{214}Pb vs ^{212}Pb, the correlation is not so good since the isotopes belong to different series that are not linked to each other, namely the natural decay series of ^{238}U and ^{232}Th. Even if the scattering of the activity concentration values between the samples a not observed, since they were collected from a quite wide geographical area, a kriging procedure has been applied to the results to identify the possible accumulation of contamination in a given area. The measured results have been fed to the Surfer® software, and contour maps have been drawn. Fig. 7 (a, b, c, and d) show the contour maps for activity concentration of (^{214}Bi, ^{214}Pb, ^{226}Ra, and ^{234}Th), (^{235}U), (^{208}Tl, ^{212}Bi, ^{212P}b, and ^{228}Ac), and (^{40}K), respectively.

Table (4): The radioactivity level of related work for similar lakes in Egypt and others worldwide

Invistigated area	U-238	Th-232	K-40	Cs-137
	Activity Concentration (Bq/kg)			
Present work	20.2 (4.3-47.5)	14.8 (1.9-7.3)	285.8 (127.6 -409.1)	ND
Mariout Lake, Egypt [35]	12.65 (10.52 –15.91)	7.24 (544–8.33)	518.75 (441.64– 582.31)	3.68 (2.30–4.20)
Brullus Lake, Egypt [35]	17.26 (12.60 –19.90)	10.03 (8.50–10.60)	299.7 (258.87– 316.80)	3.33 (2.4 –3.90)
Brullus Lake, Egypt [36]	14.3 (10.3–21.8)	20.0 (11.9–34.4)	312 (268– 401)	7.2 (2.7 –15.9)
Idku Lake, Egypt [37]	20.37 (11.19 –39.33)	26.05 (11.4–43.31)	329.05 (163.05– 507.95)	1.22 (0.4 –4.29)
Idku Beach, Egypt [37]	13.08 (5.53–27.45)	13.97 (5.48–36.93)	345.97 (239.07– 496.85)	0.48 (0.14–496.85)
Red Sea, Egypt [38]	24.6 (5.2 –105.6)	31.4 (2.3 –221.9)	428 (98– 1011)	ND
Nasser Lake, Egypt [39]	14.3 –22.0	18.4 –24.4	222– 326	2.3–7.6
Gulf, Saudi Arabia [40]	16.97 (8.68–37.20)	22.48 (5.28–58.87)	641.08 (324.55– 1133.04)	3.47 (0.0 –8.65)
Butrint Lagoon, Albania [41]	13.0 –26.6	13.1-38.1	266– 675	2.8–37.5

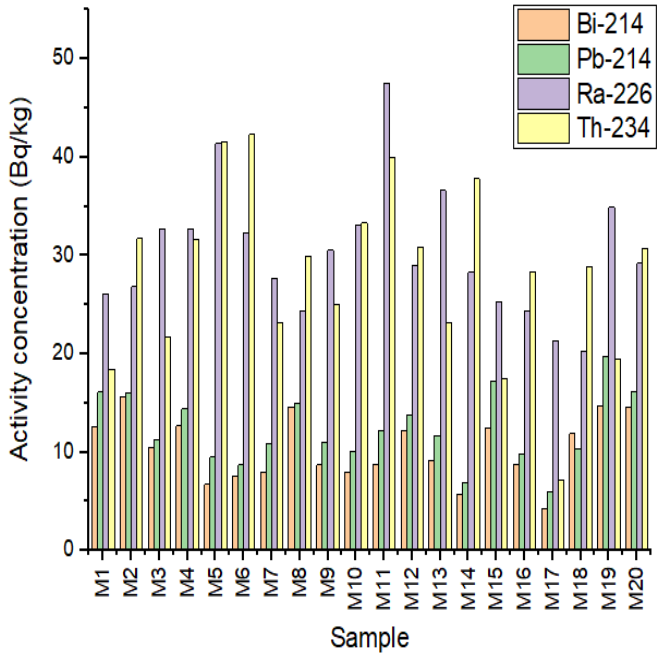

Fig. (2): The activity concentration of ^{238}U gamma-emitting daughter nuclides (^{214}Bi, ^{214}Pb, ^{226}Ra, ^{234}Th)

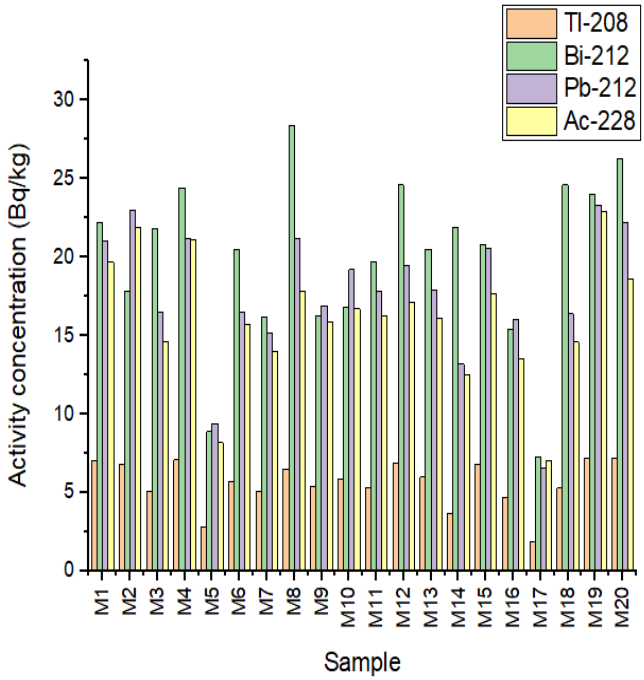

Fig. (3): The activity concentration of ^{232}Th gamma-emitting daughter nuclides (^{208}Tl, ^{212}Bi, ^{212}Pb, ^{228}Ac)

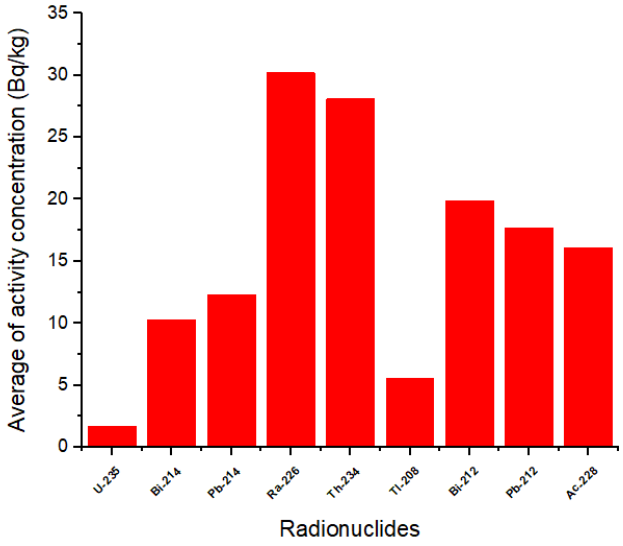

Fig. (4): The comparison between the average values of the activity concentration of ^{235}U, ^{238}U, ^{232}Th gamma-emitting radionuclides

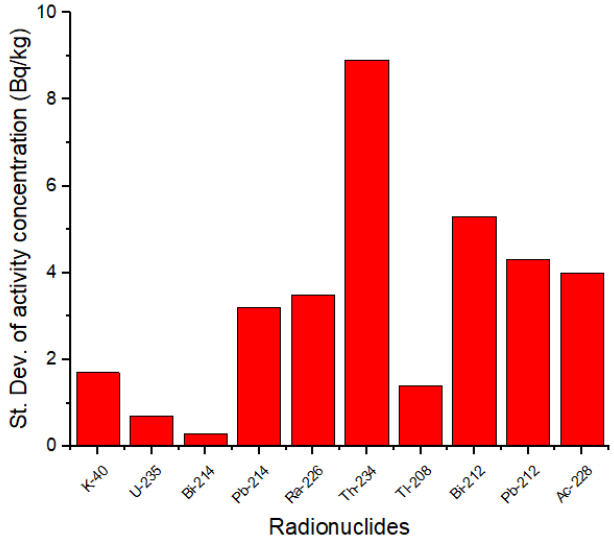

Fig. (5): The comparison between the standard deviation values of the activity concentration of ^{235}U, ^{238}U, ^{232}Th gamma-emitting radionuclides

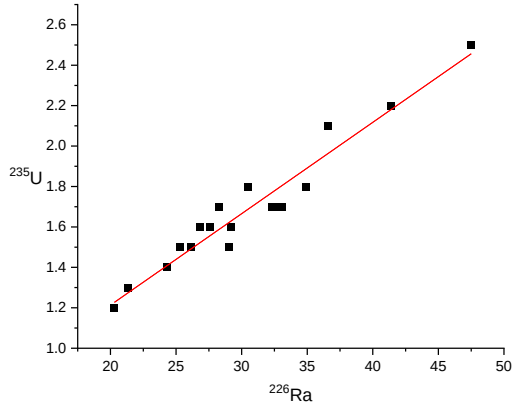

Fig. 6 (a): The correlation relation between the activity concentration of ^{226}Ra and ^{235}U

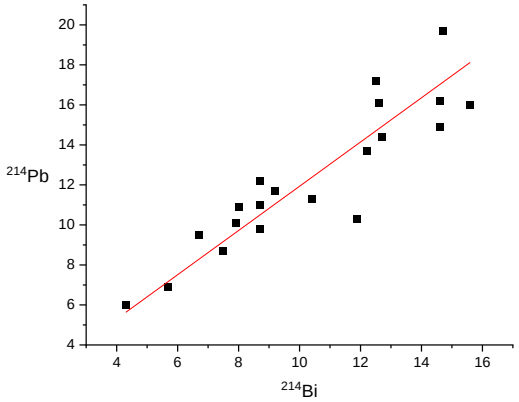

Fig. 6 (b): The correlation relation between the activity concentration of ^{214}Bi and ^{214}Pb

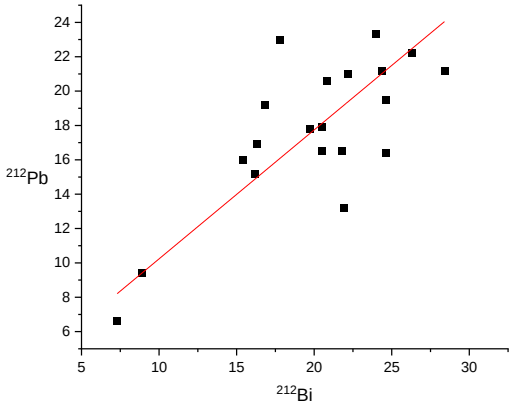

Fig. 6 (c): The correlation relation between the activity concentration of ^{212}Bi and ^{212}Pb

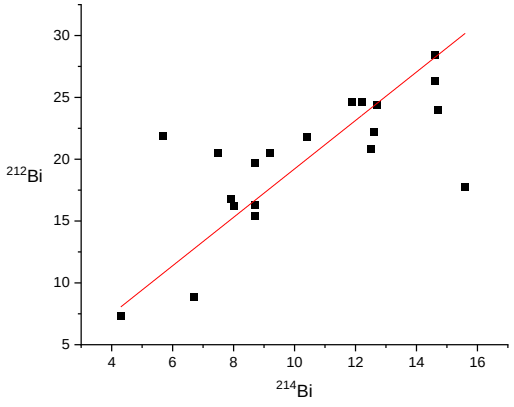

Fig. 6 (d): The correlation relation between the activity concentration of ^{214}Bi and ^{212}Bi

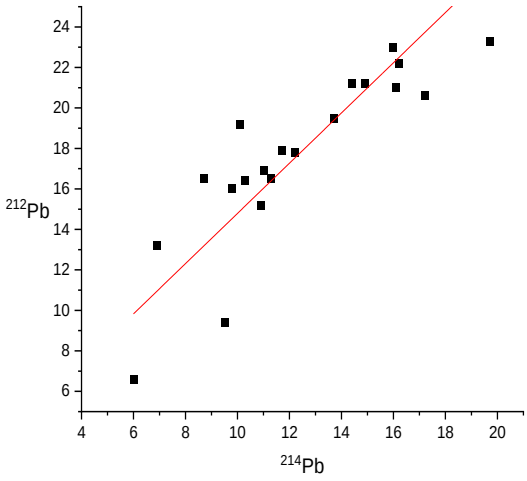

Fig. 6 (e): The correlation relation between the activity concentration of ^{214}Pb and ^{212}Pb

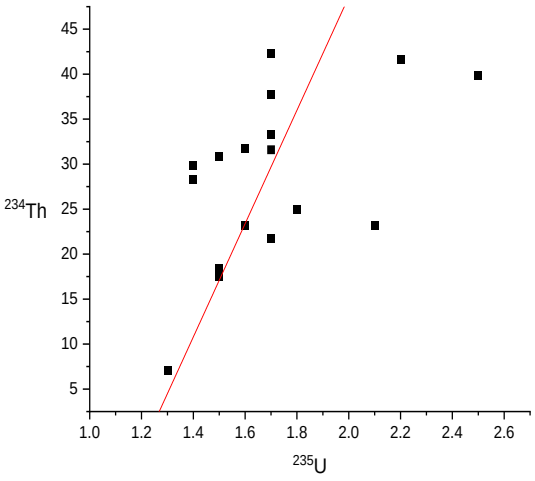

Fig. 6 (f): The correlation relation between the activity concentration of ^{235}U and ^{234}Th

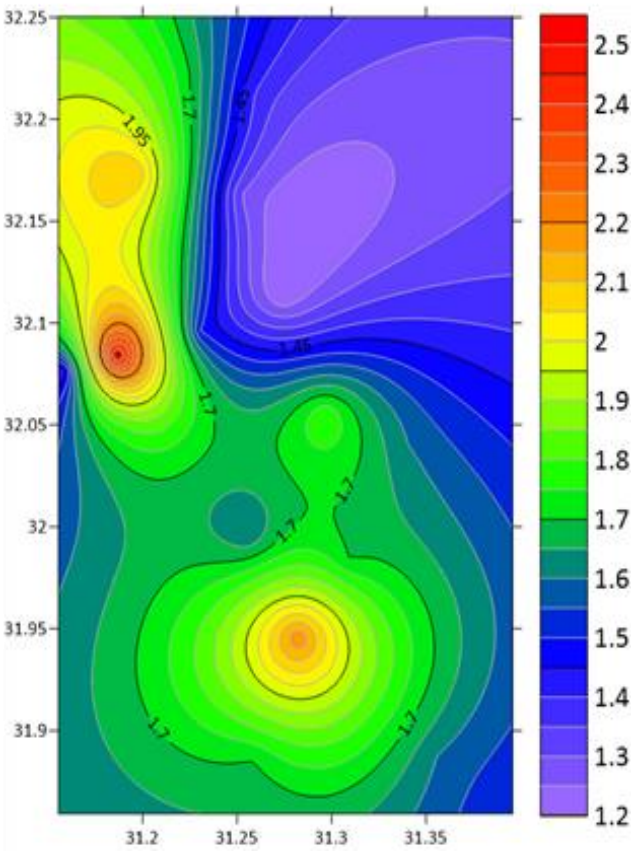

Fig. 7 (a): Contour map for the overall average of (^{214}Bi, ^{214}Pb, ^{226}Ra, and ^{234}Th) activity concentration (Bq/kg)

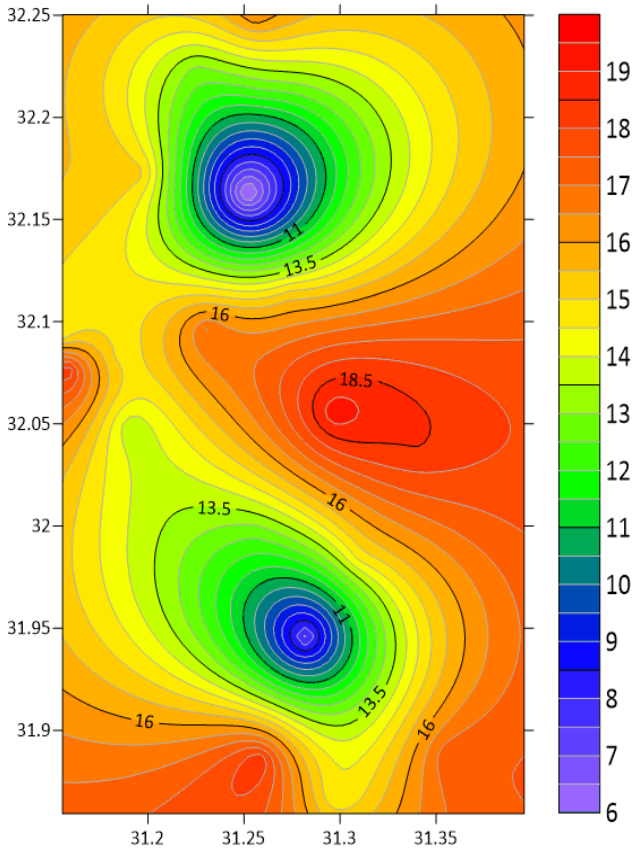

Fig. 7 (b): Contour map for the overall average of (^{208}Tl, ^{212}Bi, ^{212}Pb, and ^{228}Ac) activity concentration (Bq/kg)

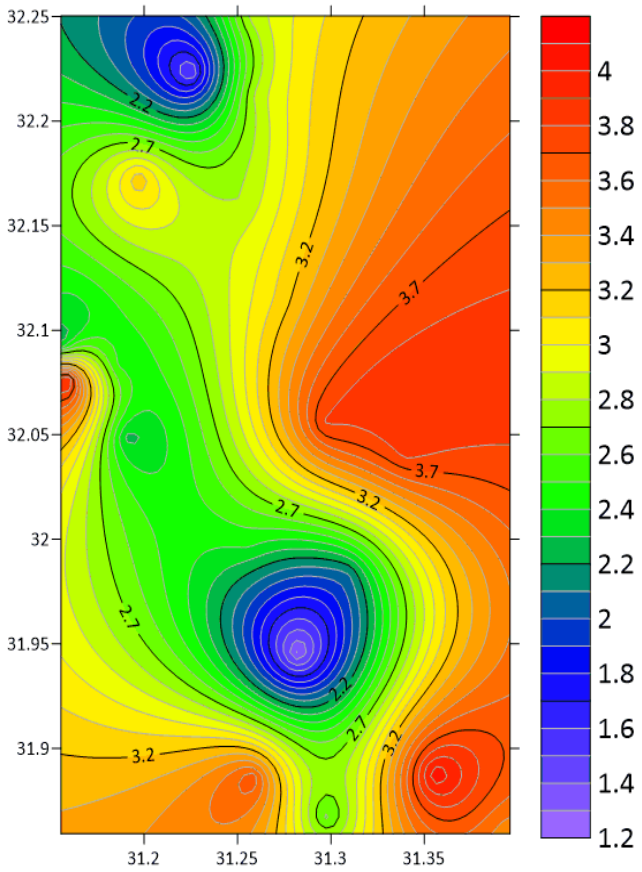

Fig. 7 (c): Contour map for the overall average of ^{40}K activity concentration (Bq/kg)

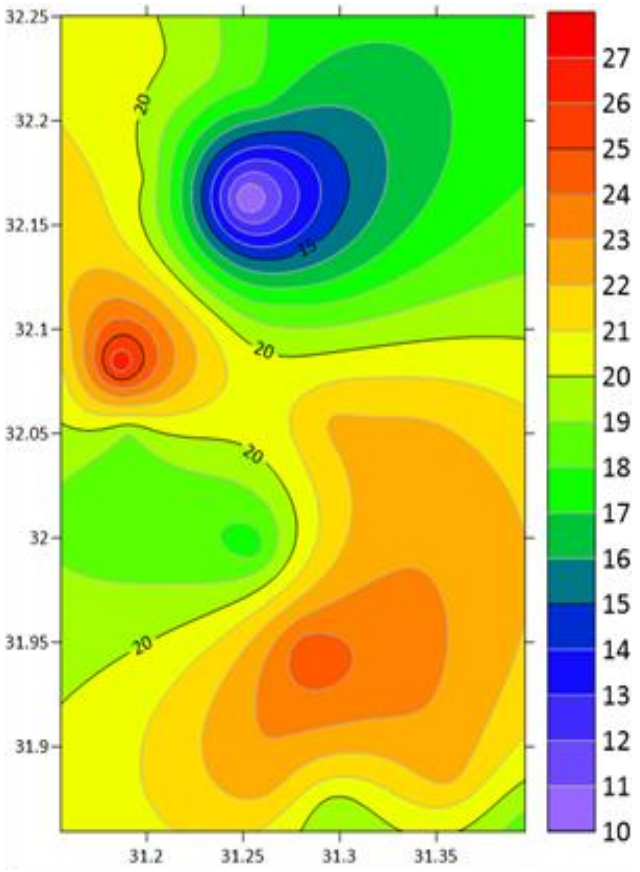

Fig. 7 (d): Contour map for the overall average of ^{235}U activity concentration (Bq/kg)

CONCLUSION

Conducting the present radiological survey of the studied areas is important in order to perform an assessment of the radiological health hazards under normal circumstances and for the identification of the areas that are more polluted and potentially more due to agricultural and industrial activities and municipal wastewater effluents. The obtained data could help in detecting any change of the radioactive background level as a consequence of geological processes, and may serve as reference information for Lake Manzala to detect the presence of harmful radiation that might affect the workers and fish farms, and agricultural farmland that depends on the Lake as a permanent source of water. The obtained contour maps are useful when tracking any changes in the environmental radioactivity by observing the distribution of radionuclides and their activity concentration. It is noticeable that the results will be used in the future to complete the baseline data concerning the periodic radiological protection and environmental radioactivity monitoring for Egyptian lakes.

ACKNOWLEDGMENTS

The authors would like to thank Mr. Aymen Magdy (Nuclear and Radiation Research Group, Faculty of Science, Mansoura University) for his collaboration and help in collecting the samples from the investigated areas. In addition, the authors express their thanks to the researchers in the Radiation Protection Department, Institute for Nuclear Research (RATEN-ICN) Romania, for helping in the needed measurements of the gamma-ray spectrometer (HPGe).

Data availability statements

The dataset containing the activity concentrations of gamma-emitting radionuclides identified in the sediment samples from Lake Manzala are included in the current article. Moreover, all the analyzed spectra and true coincidence summing corrections have been applied using the Genie-2000 software and LabSOCS, respectively, and the database profile is available with the corresponding author.

REFERENCES

[1] IAEA, *Radiation Protection against Radon in Workplaces other than Mines*. 2004, Vienna: INTERNATIONAL ATOMIC ENERGY AGENCY.

[2] Ongori, J.N., et al., *Determining the radon exhalation rate from a gold mine tailings dump by measuring the gamma radiation.* J Environ Radioact, 2015. **140**: p. 16-24.

[3] Saleh, G.M., et al., *Environmental Radioactivity of Radon and its Hazards in Hamash Gold Mine, Egypt.* Arab Journal of Nuclear Sciences and Applications, 2019. **52**(4): p. 190-196.

[4] UNSCEAR, *Sources and Effects of Ionizing Radiation*, ed. R.t.t.G. Assembly. Vol. 1. 2000, New York: United Nations Scientific Committee on the Effects of Atomic Radiation.

[5] Abbas, Y.M., et al., *Measurement of 226Ra concentration and radon exhalation rate in rock samples from Al-Qusair area using CR-39.* Journal of Radiation Research and Applied Sciences, 2020. **13**(1): p. 102-110.

[6] Ahmad, N., M.S. Jaafar, and S.A. Khan, *Correlation of radon exhalation rate with grain size of soil collected from Kedah, Malaysia.* Sci. Int, Lahore, 2014. **26**(2): p. 691-696.

[7] IAEA, *Analytical Methodology for the Determination of Radium Isotopes in Environmental Samples*. 2011, Vienna: International Atomic Energy Agency.

[8] IAEA, *Nuclear Data for the Production of Therapeutic Radionuclides*. 2012, Vienna: International Atomic Energy Agency.

[9] ICRP, *Protection Against Radon-222 at Home and at Work*. 1993, ICRP. p. . Ann. ICRP 23 (2).

[10] UNSCEAR, *Report of the United Nations Scientific Committee on the Effects of Atomic Radiation* UNSCEAR, 2011. **58**: p. 12.

[11] Zhuo, W., et al., *Estimating the amount and distribution of radon flux density from the soil surface in China.* J Environ Radioact, 2008. **99**(7): p. 1143-8.

[12] Kathren, R.L., *Radioactivity in the environment : sources, distribution, and surveillance*. 1984: Harwood Academic Publishers.

[13] Dragović, S. and A. Onjia, *Classification of soil samples according to their geographic origin using gamma-ray spectrometry and principal component analysis.* Journal of Environmental Radioactivity, 2006. **89**(2): p. 150-158.

[14] Zahran, M.A.E.-K., et al., *Assessment and distribution of heavy metals pollutants in Manzala Lake, Egypt.* Journal of Geoscience and Environment Protection, 2015. **3**(06): p. 107.

[15] Yamashita, N., et al., *Organochlorine pesticides in water, sediment and fish from the Nile River and Manzala Lake in Egypt.* International Journal of Environmental Analytical Chemistry, 2000. **77**(4): p. 289-303.

[16] Hereher, M.E., *The Lake Manzala of Egypt: an ambiguous future.* Environmental Earth Sciences, 2014. **72**(6): p. 1801-1809.

[17] Hussein M. Rashad, a.A.M.A.-A., *Lake Manzala, Egypt: A Bibliography.* Assiut Univ. J. of Botany, 2010. **39**(1): p. 253-289.

[18] Rashed, A., et al. *Env ironmental protection of Lake Manzala, Egypt and reuse of treated water by a constructed wetland*. in *International Workshop on Development and Management of Flood Plains and Wetlands (IWFW), Beijing, China*. 2000.

[19] Randa R. Elmorsi, K.S.A.-E.-S., Gamal Abdel-Hafiz Mostafa, Mohamed A. Hamed, *Distribution of essential heavy metals in the aquatic ecosystem of Lake Manzala, Egypt.* Heliyon, 2019. **5**(8).

[20] Vandenhove, H., C. Gil-García, A. Rigol, M. Vidal, *New best estimates for radionuclide solid–liquid distribution coefficients in soils. Part 2. Naturally occurring radionuclides.* Journal of Environmental Radioactivity, 2009. **100**(9): p. 697-703.

[21] IAEA, *Soil Sampling for Environmental Contaminants*. 2004, Vienna: International Atomic Energy Agency.

[22] Olley, J.M., A. Murray, and R.G. Roberts, *The effects of disequilibria in the uranium and thorium decay chains on burial dose rates in fluvial sediments.* Quaternary Science Reviews, 1996. **15**(7): p. 751-760.

[23] Tripathi, R.M., et al., *Study of uranium isotopic composition in groundwater and deviation from secular equilibrium condition.* Journal of Radioanalytical and Nuclear Chemistry, 2013. **295**(2): p. 1195-1200.

[24] Todd, D.K. and L.W. Mays, *Groundwater hydrology*. 2004: John Wiley & Sons.

[25] Ivanovich, M., *Uranium series disequilibrium: applications to environmental problems*. 1982: Clarendon Press.

[26] EPA, *External Exposure to Radionuclides in Air, Water, and Soil*, in *EPA Federal Guidance Report*. 1993, Environmental Protection Agency: Washington. p. 238.

[27] Barooah, D. and P.P. Gogoi, *Study of radium content, radon exhalation rates and radiation doses in solid samples in coal-mining areas of Assam and Nagaland using LR-115 (II) nuclear track detectors*. 2019, India: Vishal Publishing Company.

[28] El-Farrash, A.H., H.A. Yousef, and A.F. Hafez, *Activity concentrations of 238U and 232Th in some soil and fertilizer samples using passive and active techniques.* Radiation Measurements, 2012. **47**(8): p. 644-648.

[29] Mahur, A.K., et al., *Measurement of natural radioactivity and radon exhalation rate from rock samples of Jaduguda uranium mines and its radiological implications.* Nuclear Instruments and Methods in Physics Research Section B: Beam Interactions with Materials and Atoms, 2008. **266**(8): p. 1591-1597.

[30] Shafi ur, R., et al., *Determination of 238U contents in ore samples using CR-39-based radon dosimeter—disequilibrium case.* Radiation Measurements, 2006. **41**(4): p. 471-476.

[31] Hashim, A.K. and L.A. Najam, *Measurement of uranium concentrations, radium content and radon exhalation rate in iraqian building materials samples.* International Journal of Physics, 2015. **3**(4): p. 159-164.

[32] L'Annunziata, M.F., *Nuclear radiation, its interaction with matter and radioisotope decay*. Handbook of Radioactivity Analysis, 2003: p. 1-122.

[33] IAEA, *National and Regional Surveys of Radon Concentration in Dwellings*. 2014, Vienna: International Atomic Energy Agency.

[34] IRSN, *Natural Uranium and the environment: appendices*, B. Bonin, Editor. 2012, nstitut de radioprotection et de sûreté nucléaire.

[35] Dar, M.A. and A.A. El Saharty, *Activity levels of some radionuclides in Mariout and Brullus lakes, Egypt.* Radiation Protection Dosimetry, 2013. **157**(1): p. 85-94.

[36] El-Reefy, H.I., et al., *Distribution of gamma-ray emitting radionuclides in the marine environment of the Burullus Lake: II. Bottom sediments.* Environmental Monitoring and Assessment, 2010. **169**(1): p. 273-284.

[37] Fahmi, N., et al., *Study of the environmental impacts of the natural radioactivity presents in beach sand and Lake Sediment samples Idku, Behara, Egypt.* 2011.

[38] El Mamoney, M. and A.E. Khater, *Environmental characterization and radio-ecological impacts of non-nuclear industries on the Red Sea coast.* Journal of Environmental Radioactivity, 2004. **73**(2): p. 151-168.

[39] Khater, A.E., Y.Y. Ebaid, and S.A. El-Mongy. *Distribution pattern of natural radionuclides in Lake Nasser bottom sediments*. in *International Congress Series*. 2005. Elsevier.

[40] Al-Trabulsy, H., A. Khater, and F. Habbani, *Radioactivity levels and radiological hazard indices at the Saudi coastline of the Gulf of Aqaba.* Radiation Physics and Chemistry, 2011. **80**(3): p. 343-348.

[41] Tsabaris, C., et al., *Radioactivity levels of recent sediments in the Butrint Lagoon and the adjacent coast of Albania.* Applied Radiation and Isotopes, 2007. **65**(4): p. 445-453.